POLITECNICO DI TORINO
Repository ISTITUZIONALE

All-Metal Connected-Element Arrays for LEO Orbits in Ka-Band

Original
All-Metal Connected-Element Arrays for LEO Orbits in Ka-Band / Vazquez-Sogorb, C., Montoya-Roca, R., Paonessa, F., Addamo, G., Peverini, O.A., Maiarelli, D., Gasparro, G., Virone, G.. - ELETTRONICO. - (2026), pp. 1-4. (2026 20th European Conference on Antennas and Propagation (EuCAP) Dublin (Ire) 19-24 April 2026) [10.23919/eucap68105.2026.11612538].

Availability:
This version is available at: 11583/3015050 since: 2026-11-17T10:08:36Z

Publisher:
IEEE

Published
DOI:10.23919/eucap68105.2026.11612538

Terms of use:

This article is made available under terms and conditions as specified in the corresponding bibliographic description in the repository

Publisher copyright
IEEE postprint/Author's Accepted Manuscript

©2026 IEEE. Personal use of this material is permitted. Permission from IEEE must be obtained for all other uses, in any current or future media, including reprinting/republishing this material for advertising or promotional purposes, creating new collecting works, for resale or lists, or reuse of any copyrighted component of this work in other works.

(Article begins on next page)

29 November 2026

All-Metal Connected-Element Arrays for LEO Orbits in Ka-Band

C. Vazquez-Sogorb*†, R. Montoya-Roca*†, F. Paonessa†, G. Addamo†,
O. A. Peverini†, D. Maiarelli*, G. Gasparro*, G. Virone†

*Thales Alenia Space, Roma, Italy, carlos.vazquez@thalesaleniaspace.com
†IEIIT - National Research Council of Italy (CNR), Turin, Italy, carlos.vazquezsogorb@ieiit.cnr.it

***Abstract*—This paper presents a compact six-ridged hexagonal waveguide aperture with integrated grooves, developed for Ka-band transmit array applications within the framework of next-generation non-terrestrial networks. The proposed design combines sixfold geometric symmetry with a continuous groove structure to enhance polarization stability, reduce inter-element coupling, and maintain broadband impedance matching over wide scanning angles. The aperture operates efficiently across the 17.7–20.2 GHz band, achieving reflection and coupling levels below –10 dB, scan loss under 3 dB up to 50°, and cross-polarization discrimination above 15 dB up to 60°. A seven-element cluster implementation validates the element's robustness and wide-angle performance. Results confirm the suitability of the proposed aperture for compact, high-efficiency Ka-band phased arrays in satellite communication payloads.**

***Index Terms*—Ka-band antennas, waveguide apertures, phased arrays, mutual coupling, satellite communications.**

I. Introduction

The next generation of communication networks, particularly sixth-generation (6G) systems, aims to extend global connectivity by integrating non-terrestrial networks (NTNs), which encompass various satellite platforms that provide broadband access in remote or underserved regions, with terrestrial infrastructure. Among them, low Earth orbit constellations have attracted remarkable interest due to their lower latency and propagation losses compared to medium and geostationary orbits [1]. Next-generation satellite payloads must provide multiple high-gain beams over a wide field of view while ensuring polarization purity, beam agility, and robustness to misalignments. Achieving these features requires careful aperture design to balance element size, radiation efficiency, and manufacturability.

Several radiating elements have been explored for Ku- and Ka-band arrays, such as microstrip patches [2], Vivaldi antennas [3], and waveguide apertures [4], [5]. Among them, metallic waveguide-fed structures are favored in high-power front-ends due to their low losses and thermal stability. To enable compact apertures and wide-angle scanning, ridge-loaded waveguides are often employed, as they lower the cut-off frequency and can be designed to support dual-mode operation for circular polarization. In this context, multi-ridge configurations, particularly six-ridged hexagonal geometries, offer enhanced symmetry and improved polarization performance near broadside [6].

In dense waveguide arrays, strong mutual coupling between adjacent apertures can degrade impedance matching, distort the radiation pattern, and reduce overall array efficiency. These couplings become more pronounced as the inter-element spacing approaches half a wavelength, often leading to scan blindness [7]. To mitigate these effects, several techniques have been proposed, such as grouping elements into subarrays to modify the overall periodicity [8]—though this can reduce the radiation efficiency due to the loss of power to grating lobes—directly altering the inter-element spacing [9], or suppressing surface waves through defected ground structures [5] or electromagnetic bandgap surfaces operating within their stopband. Moreover, beyond the scan blindness phenomenon typically observed in quasi-infinite arrays, the active reflection coefficient also varies with the scan angle as a result of mutual coupling [10]. To compensate for this behavior, wide-angle impedance matching techniques are often employed, although they can degrade array performance at large scan angles [11]. Overall, effective management of mutual coupling is essential to ensure stable performance across wide scanning ranges and to preserve polarization purity and gain uniformity in large-scale phased arrays.

This paper presents a compact six-ridged hexagonal waveguide aperture with integrated grooves, specifically developed for Ka-band transmit array applications. The proposed element combines sixfold geometric symmetry with a groove profile to enhance polarization stability, minimize mutual coupling, and maintain efficient radiation across wide scanning angles. The design is validated through a seven-element cluster that incorporates a dual-port end-launcher, a compact circular polarizer and a bed-of-nails layer used to emulate infinite-array conditions [12]. Full-wave analysis demonstrates proper operation within the 17.7–20.2 GHz frequency range, supporting scan angles up to 60°, with grating-lobe suppression, return loss greater than 10 dB, scan loss under 3 dB, and cross-polarization discrimination (XPD) above 15 dB at the maximum scan angle of 60°.

The paper is structured as follows: Section II describes the electromagnetic design and coupling analysis of the proposed six-ridged hexagonal aperture. Section III details its integration within a finite cluster including the bed-of-nails environment. Section IV summarizes the key performance outcomes and design implications for Ka-band phased arrays.

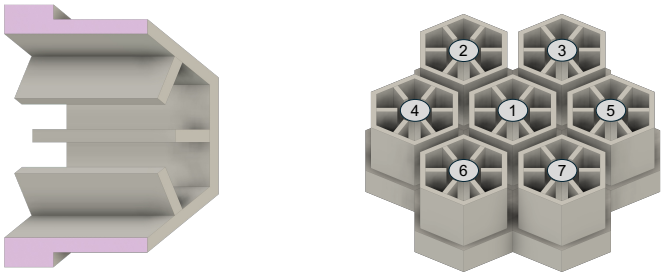

(a) Element cross-section (b) 7-element cluster

Fig. 1. Six-ridged hexagonal grooved waveguide aperture

II. Aperture Element Design

The aperture element, whose cross-section is shown in Fig. 1a, has been designed with a periodicity that guarantees grating-lobe-free operation across the Ka-band for scan angles up to 60°, 0.62λ mm, assuming a triangular lattice arrangement. To prevent the cut-off frequency of the grating-lobe at the maximum frequency of the operating band and maximum scanning angle, the inter-element spacing was computed considering an additional safety margin of 500 MHz.

The effect of groove depth on the six-ridged hexagonal aperture was analyzed through the active reflection coefficient across multiple scan angles. Results indicate that a groove depth close to a quarter-wavelength at the central frequency provides optimal matching and enhanced inter-element isolation, with significant performance across scanning directions.

The impact of the surrounding continuous groove was also evaluated in a finite seven-element cluster (Fig. 1b). Simulation results show that the central element primarily defines the resonant response, with the resonance centered within the band and slightly improved matching at higher frequencies for both fundamental modes (orange solid line in Figs. 2 and 3). Regarding the first mode, whose dominant electric field is oriented along the horizontal axis, the groove effectively reduces coupling toward diagonally aligned elements, while its influence on horizontally ones remains limited (Fig. 2). In contrast, for the second mode polarized along the vertical axis, noticeable improvement is only observed for horizontally aligned elements at low frequencies, showing no significant effect at higher ones (Fig. 3). Further details regarding the groove performance depending on mode polarization and ridge orientation within the cavity will be discussed at the conference.

Moreover, the simulations show that the proposed aperture exhibits stable impedance performance across the full scan range, with both active reflection and coupling coefficients remaining below −10 dB. Owing to its sixfold symmetry and continuous groove structure, no additional matching network is required to ensure broadband impedance stability. The co-polarized gain (Fig. 4) remains stable across the operating band and scan angles, with losses below 3 dB up to 50° and about 5 dB at the lowest frequency and widest scan. The six-ridge geometry provides nearly symmetric LHCP and RHCP

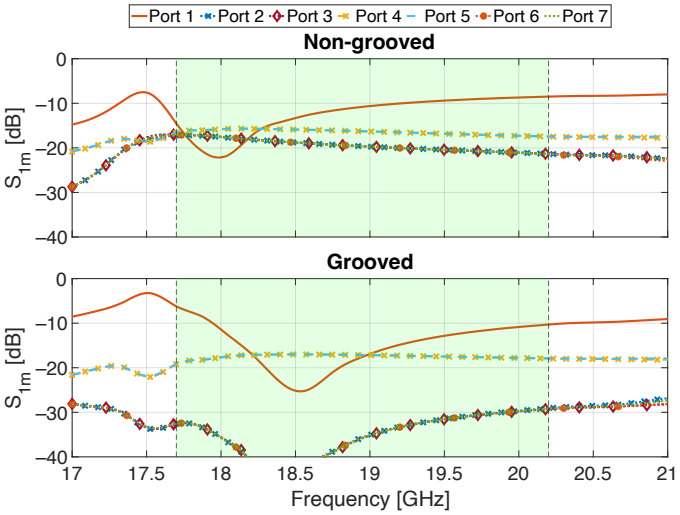

Fig. 2. Finite array simulation of the S_{11} at the central element (Port 1) and mutual coupling of the other elements (Ports 2 to 7) to the central one scanning at broadside in a 7-element cluster. The top figure considers a design without isolation. The bottom figure considers a continuous groove between elements. The green box indicates the operative frequency band.

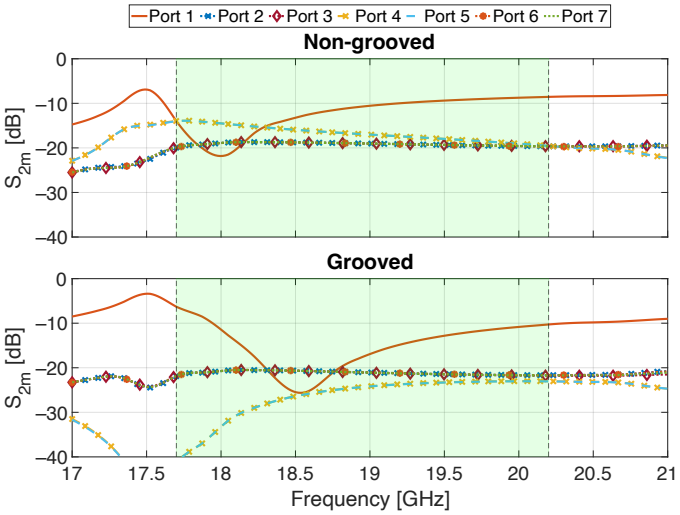

Fig. 3. Finite array simulation of the S_{22} at the central element (Port 1) and mutual coupling of the other elements (Ports 2 to 7) to the central one scanning at broadside in a 7-element cluster. The top figure considers a design without isolation. The bottom figure considers a continuous groove between elements. The green box indicates the operative frequency band.

responses in all principal planes, with minor deviations under extreme scans. XPD exceeds 15 dB at the maximum scan angle, and the aperture achieves a broadside directivity of 5.4 dBi at the central frequency, consistent with compact Ka-band apertures.

III. Array Environment Design

To properly assess the performance of the proposed radiating element, it has been embedded within a finite seven-element array arranged in a hexagonal configuration, with a central aperture surrounded by six identical elements. However, due to the finite nature of this setup, edge effects can

significantly influence the impedance and radiation behavior of the embedded element. These effects arise from the lack of periodic boundary conditions, leading to non-uniform field distributions and modified coupling levels compared to an infinite array environment.

To address this issue, different boundary configurations were analytically evaluated. When the surrounding region is left as free space, noticeable degradation occurs, with more than 3 dB loss at lower frequencies under broadside conditions. Replacing this area with a continuous metallic region extending up to the aperture plane yields moderate improvement at these frequencies but introduces additional attenuation at higher ones, particularly under wide-angle scanning.

As an effective mitigation strategy, a peripheral bed of metallic pins forming a high-impedance bed-of-nails (BON) surface with a slight height increase of around $\lambda/10$ above the aperture plane, has been implemented to emulate infinite-array conditions [12], [13]. This structure provides a high-impedance boundary at the aperture plane, effectively suppressing backward radiation and enhancing overall antenna gain [14], [15]. When designed to slightly extend above the aperture plane, the BON configuration achieves a balanced trade-off across the operating band, resulting in a smoother spectral response and improved co-polarized radiation for all scan angles. This validates its capability to accurately reproduce the electromagnetic behavior of an element embedded in an infinite array.

Fig. 5 presents the simulated realized gain at the maximum frequency of the operating band for the embedded central element, with all surrounding elements properly matched. The co-polarized component (solid lines) exhibits slightly lower values than the scan loss trend of $\cos^{1.4}(\theta)$. The cross-polarized component shows an XPD greater than 10 dB at $\phi = 90°$ and $\theta = 60°$ (blue curve).

Fig. 6 presents the simulated and measured Axial Ratio (AR) at the central frequency of the operating band for the embedded central element, with all reamining elements properly matched. Although the simulation (dashed lines) and experimental results (solid lines) exhibit similar trends, minor deviations occur near broadside. The AR maintains proper circular polarization with values below 3 dB over a 120° field of view.

In addition, both simulated and experimental results will be presented at the conference to validate key performance metrics of the proposed cluster.

IV. Conclusions

A compact six-ridged hexagonal grooved waveguide aperture for Ka-band transmit arrays has been presented and validated. The design achieves stable impedance performance, low mutual coupling, and robust circular polarization across the 17.7–20.2 GHz band, supporting scan angles up to 60°. The element maintains reflection and coupling below –10 dB, scan loss below 3 dB, and XPD above 15 dB. Embedding the element in a seven-element cluster with a high-impedance bed-of-nails surface effectively emulates infinite-array conditions,

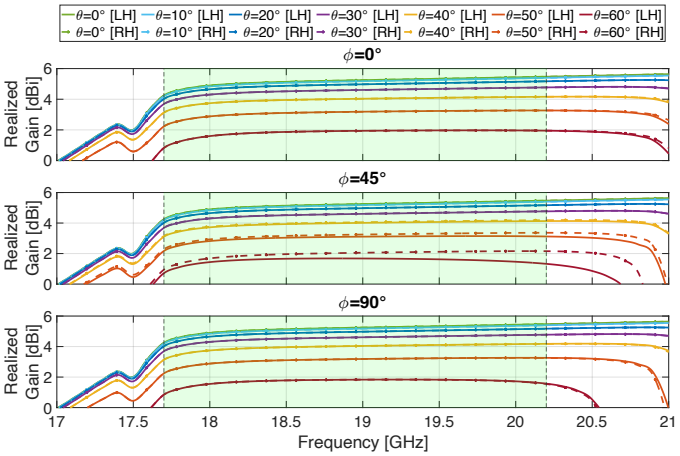

Fig. 4. Simulated radiation pattern of the aperture element in an unit-cell environment at $\phi = 0°/45°/90°$ for $0° < \theta < 60°$ angles. Solid lines indicates left-hand circular polarization. Dashed lines indicates right-hand circular polarization. The green box indicates the operative frequency band.

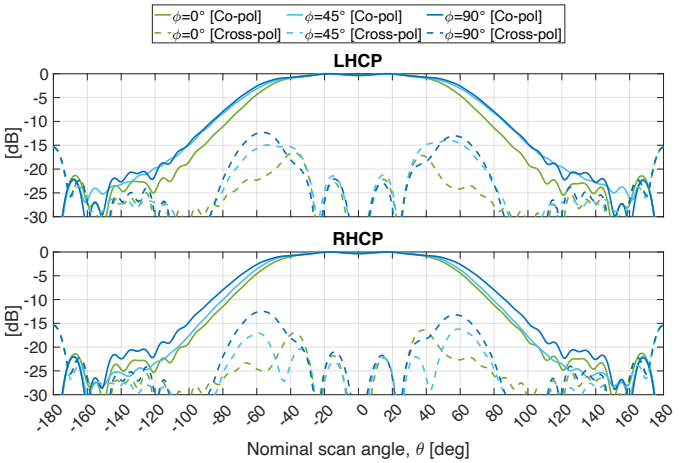

Fig. 5. Simulated normalized embedded radiation pattern of the 7-element cluster at 20.2 GHz for several planes.

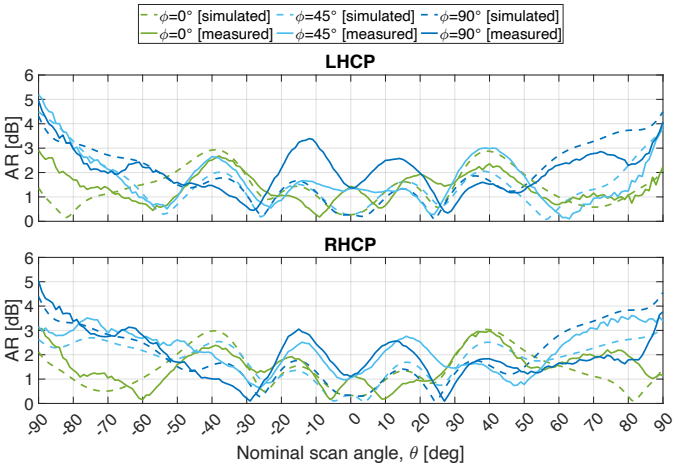

Fig. 6. Measured and simulated Axial Ratio of the 7-element cluster at the central frequency for several planes.

enhancing gain and suppressing grating lobes. These results confirm the suitability of the proposed aperture for compact, wide-angle Ka-band satellite arrays.

ACKNOWLEDGMENT

Funded by the European Union, under ANTERRA 101072363 HORIZON-MSCA-2021-DN-01. Views and opinions expressed are however those of the author(s) only and do not necessarily reflect those of the European Union. Neither the European Union nor the granting authority can be held responsible for them.

REFERENCES

[1] Giordani, M.; Zorzi, M. Non-Terrestrial Networks in the 6G Era: Challenges and Opportunities. *IEEE Netw.* **2021**, *35*, 244–251.

[2] K. -X. Li, Z. -J. Guo and Z. -C. Hao. A Multipolarized Planar Phased Array for LEO SATCOM Applications. *IEEE Antennas and Wireless Propagation Letters* **2022**, *21*, 2273–2277.

[3] H. Kähkönen, J. Ala-Laurinaho and V. Viikari. A Modular Dual-Polarized Ka-Band Vivaldi Antenna Array. *IEEE Access* **2022**, *10*, 36362–36372.

[4] Polo-López, L.; Menargues, E.; Capdevila, S.; Toso, G.; García-Vigueras, M. Solving Sub-Wavelength Lattice Reduction in Full-Metal Front-Ends for Dual-Polarized Active Antennas. *IEEE Trans. Antennas Propag.* **2022**, *70*, 7413–7426.

[5] Polo-López, L.; Berretti, L.; Menargues, E.; Capdevila, S.; Toso, G.; García-Vigueras, M. Dual-polarized Spaceborne Phased Arrays Using Tri-Ridge Evanescent Waveguide Antennas. *IEEE Antennas and Wireless Propagation Letters* **2024**, *18*, 1–5.

[6] Vazquez-Sogorb, C.; Montoya-Roca, R.; Addamo, G.; Peverini, O.A.; Virone, G. Ridged Apertures for LEO Direct Radiating Arrays in Ka-Band. *Appl. Sci* **2024**, *14*.

[7] Pozar, D. M; Schaubert, D. Scan blindness in infinite phased arrays of printed dipoles. *IEEE Trans. Antennas Propag.* **1984**, *32*, 602–610.

[8] Pozar, D. M. Scanning characteristics of infinite arrays of printed antenna subarrays. *IEEE Trans. Antennas Propag.* **1992**, *40*, 666–674.

[9] Harms, S.; De Kok, M.; Monni, S.; Garufo, A; Fraysse. J.; Girard, T.; Johannsen, U. Waveguide Antenna Array Element with Minimized Power Amplifier Load Pull for LEO NTNs. In Proceedings of the 2024 54th European Microwave Conference (EuMC), Paris, France. September 2024.

[10] Wheeler, H. Simple relations derived fom a phased-array antenna made of an infinite current sheet. *IEEE Trans. Antennas Propag.* **1965**, *13*, 506–514.

[11] Magill, E.; Wheeler, H. Wide-angle impedance matching of a planar array antenna by a dielectric sheet. *IEEE Trans. Antennas Propag.* **1996**, *14*, 49–53.

[12] Chernikov, V.; Vilenskiy, A.; Agneessens, S.; Manholm, L.; Kehn, M. N. M.; Ivashina, M. A Teflon-Filled Open-Ended Circular Waveguide Focal-Plane-Array Used for Sway Compensation in W-band 50dB-Gain Backhaul Reflector Antennas. In Proceedings of the 2023 International Conference on Electromagnetics in Advanced Applications (ICEAA), Venice, Italy. October 2023.

[13] Chernikov, V. S.; Vilenskiy, A. R.; Agneessens, S.; Manholm, L.; Ivashina, M. V. A W-Band Choke-Ring Encircled Focal Plane Array of Full-Metal Elements for Reflector Antennas With Over 50%-Efficiency High Crossover Beams. *IEEE Antennas and Wireless Propagation Letters* **2024**, *23*, 4578–4582.

[14] Ahmadfard, F.; Parizi, S. A. R. Backlobe suppressed H-plane ridge gap waveguide (RGW) horn antenna. In Proceedings of the 2017 Iranian Conference on Electrical Engineering (ICEE), Tehran, Iran. May 2017.

[15] Khadiko, N.; Alshrafi, W.; Chalermwisutkul, S.; Heberling, D. Comparison of Grating Lobe Suppression Using High Impedance Structure: EBG and BON in Phased Array Antenna. In Proceedings of the 2020 International Conference on Electrical, Communication, and Computer Engineering (ICECCE), Istanbul, Turkey. June 2020.